

BBoxMaskPose v2: Expanding Mutual Conditioning to 3D

Miroslav Purkrabek *, Constantin Kolomiiets and Jiri Matas 

Visual Recognition Group, Czech Technical University in Prague,
Technicka 2, Prague 6, 160 00, Czech Republic

*Corresponding author(s). E-mail(s): purkrmir@fel.cvut.cz;

Abstract

Most 2D human pose estimation benchmarks are nearly saturated, with the exception of crowded scenes. We introduce PMPose, a top-down 2D pose estimator that incorporates the probabilistic formulation and the mask-conditioning. PMPose improves crowded pose estimation without sacrificing performance on standard scenes. Building on this, we present BBoxMaskPose v2 (BMPv2) integrating PMPose and an enhanced SAM-based mask refinement module. BMPv2 surpasses state-of-the-art by 1.5 average precision (AP) points on COCO and 6 AP points on OCHuman, becoming the first method to exceed 50 AP on OCHuman. We demonstrate that BMP’s 2D prompting of 3D model improves 3D pose estimation in crowded scenes and that advances in 2D pose quality directly benefit 3D estimation. Results on the new OCHuman-Pose dataset show that multi-person performance is more affected by pose prediction accuracy than by detection.

The code, models, and data are available on the [project website](#).

Keywords: Human Pose Estimation, Person Detection, Instance Segmentation, Mutual Conditioning

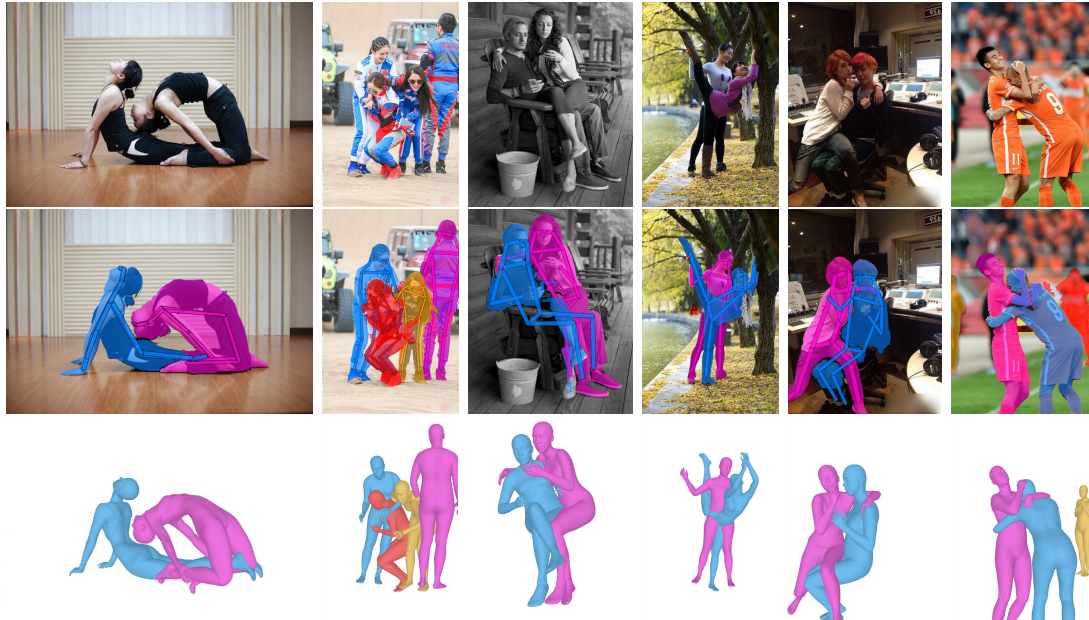


Fig. 1: **BBoxMaskPose v2** establishes a new SOTA detection, segmentation, and 2D pose estimation in crowded scenes (row 2). Combined with SAM-3D-Body [1], it enables 3D human reconstruction even in scenes with complex interactions.

1 Introduction

Human pose estimation (HPE) research is gradually shifting from 2D to 3D. However, failure cases in the wild reveal its lack of robustness even in 2D. State-of-the-art 3D pose estimators [1, 2] rely on accurate 2D input, whether from detection or prompts. Thus, improving the 2D pose estimation remains essential for reliable 3D pose estimation.

Multi-person interaction, where individuals are so close that their bounding boxes are almost the same, is one of the main challenges in 2D and 3D. Real-world data for such cases are limited [3–6]. Existing “crowded” datasets vary in difficulty – datasets such as [3–5] include individuals close to each other, but lack the interactions present in OCHuman [6].

BMPv1 [7] addresses joint detection and pose estimation in multi-person scenes and sets SOTA results on OCHuman. Its core is a self-improving loop of three lightweight models – a detector, a pose estimator, and a segmentation model – conditioned on each other to iteratively refine their predictions. While BMP improves all three tasks, it remains error-prone, particularly in the mask refinement stage. The prompting of SAM [8] within BMP is complex and often leads to over-segmentation.

This paper introduces **BMPv2**, an upgrade of BMPv1 that consistently improves pose estimation and segmentation performance. BMPv2 extends BMPv1 with two new components: PMPose and SAM-pose2seg. By incorporating these changes, BMPv2 sets a new state-of-the-art performance on both standard scenes (COCO [9]) and crowded scenes (OCHuman [6]) for pose estimation and instance segmentation. The improved mask refinement from SAM-pose2seg further enables additional refinement with PMPose, resulting in **BMPv2+**, which targets high-precision scenarios at the cost of increased computation.

PMPose is a top-down pose estimation model introduced as part of BMPv2. It unifies two recently introduced HPE models, MaskPose [7] and ProbPose [10], within a single architecture. Explicitly modeling keypoint probabilities (the core idea of ProbPose) improves limb assignment and reduces false-positive detections. Mask conditioning (the core idea of MaskPose)

helps the model disentangle individuals in multi-body scenes. PMPose outperforms existing non-iterative pose estimation methods in both standard and crowded scenes.

SAM-pose2seg, a version of SAM [8] adapted for human pose prompts, helps with over-segmentation and replaces the complex prompting. It produces higher-quality segmentation masks than SAM and significantly simplifies the prompt selection problem identified in BMPv1.

Finally, we demonstrate that stronger 2D estimates improve 3D human pose estimation using SAM-3D-Body [1]. We evaluate 3D pose estimation on the challenging multi-person scenes of OCHuman and show that robust 2D predictions are key for reliable 3D reconstruction.

In summary, the main contributions are:

1. **BMPv2** and **BMPv2+**: methods for human pose estimation and segmentation that set a new state-of-the-art on standard and crowded scenes for both tasks (Sec. 3.4).
2. **PMPose**: a 2D top-down pose estimation model outperforming non-iterative methods on standard and crowded scenes (Sec. 3.1).
3. **SAM-pose2seg**: a model for pose-guided human instance segmentation (Sec. 3.2).
4. **Analysis of 3D pose estimation** on OCHuman, a dataset of challenging scenes with closely interacting people (Sec. 5.4).
5. **OCHuman-Pose dataset**: extended annotations for OCHuman [6] (Sec. 4.1).

This work integrates contributions from ProbPose [10] (CVPR 2025), BMPv1 [7] (ICCV 2025), and SAM-pose2seg [11] (CVWW 2026), and adds new evaluations and data.

2 Related Work

Detection-Based Segmentation: The most direct approach to human instance segmentation uses a detector [12–17, 17, 18]. A detector takes an image as input and outputs instance masks and class labels. Detectors work well in scenes similar to the training data, but struggle when instances overlap heavily. Under severe occlusion, they often merge multiple people into one mask, or assign different body parts to different instances. Detecting

people in crowds is often improved with hyper-parameter tuning such as non-maximum suppression, but that results in a lot of false positives in standard non-crowd scenes. [19] proposed to suppress detection not on bounding box level but after pose estimation, which results in longer inference times since false positive detections has to first be processed by pose estimator before being suppressed.

Semantics-Aware Prompted Segmentation: Several works [20–23] inject semantics into SAM [8], similarly to our SAM-*pose2seg*. They take an image and a text prompt as input and detect and segment instances. This setting is often referred to as *open-vocabulary* or *zero-shot* segmentation. While these models capture semantics and segment entire instances, they do not provide localized cues and offer no control over which instance is chosen and, therefore, are unsuitable for iterative loops such as BMP [7].

Pose-Guided Instance Segmentation is the most specific form of prompted segmentation. The model takes an image and a detected or ground-truth human pose and segments the corresponding person. These methods specialize in humans, sacrificing the generality of open-vocabulary or generic segmenters for robustness and precise, localized control. Test-time optimization methods [24, 25] refine predictions at inference without training. While training-free, they are computationally expensive and slow at test time. Standard pose-guided human segmentation methods [6, 26–31] rely on small training datasets and thus generalize poorly, especially in crowded scenes. The closest work related to SAM-*pose2seg* is CrowdSAM [32], which builds a framework around SAM to automatically annotate bounding boxes in crowds. CrowdSAM uses SAM and DINO [33] as external tools and optimizes prompts, similar to [7]. In contrast, our SAM-*pose2seg* is end-to-end and, when used in an iterative loop, outperforms CrowdSAM, as shown already in [7].

2D Human Pose Estimation: There are two main approaches: top-down and detector-free. Detector-free can be further divided into single-stage [34–37], bottom-up [38–40] and hybrid [41].

Top-down methods [17, 42–46] use person detector to detect bounding boxes and estimate

one skeleton for each bounding box. They leverage big progress in human detection and specialize in understanding of human structure. Top-down methods are the most successful on datasets such as COCO, MPII or AIC but struggle on crowded datasets (e.g. OCHuman) due to low-quality detections. Most notably, ViTPose [42] combines multiple datasets into one strong backbone and sets a strong baseline, setting up state-of-the-art performance on most datasets. While conditioning pose estimation on bounding boxes (bbox-to-pose; standard top-down approach) is well researched, conditioning pose on masks (mask-to-pose) was explored only through MaskPose [7].

While vast majority of top-down approaches are heatmap-based, some models [47–49] predict keypoints through regression or regression-focused heatmaps [50, 51]. Important for this work is ProbPose [10] – a heatmap based method modelling the underlying probability distribution. ProbPose is the first model to estimate probabilities of keypoint being out of image along with their visibilities. As will be shown in this work, such estimates are useful for pose-guided instance segmentation in the BMP loop.

Detector-free models do not achieve SOTA performance on COCO but are superior to top-down methods on OCHuman as they are specialized in decoupling close-interaction instances. The most successful model, BUCTD [41], conditions top-down pose estimation with previously estimated keypoints from bottom-up methods. It is a pose-refinement method which has state-of-the-art results on OCHuman datasets due to its strong ability to decouple people close interactions.

Human-Centered Foundational models. The latest directions in human body modeling are foundational models [52–55]. They learn general features describing the human body that could be used for all human-related tasks such as segmentation, pose estimation etc. Most notably, Sapiens 2b [52] was trained on staggering 2M images and with 2B parameters is almost four times bigger than ViTPose-h. Even with this size, foundational models perform comparatively or worse than much smaller specialized models.

Iterative Approaches: This work builds on BBoxMaskPose loop [7]. BMP combines three specialized models into a self-improving loop

ideal for crowded and interaction-rich scenarios. While BMP set a new SOTA performance on all three tasks (detection, segmentation and 2D pose estimation), it still struggles in cases such as oversegmenting human body or merging of two individuals into the same pose. Other iterative approaches are already mentioned BUCTD [41] and IterDet [56]. IterDet detects people in crowds iteratively, similarly to BMP. This work improves BMPv1 with new pose estimation and pose-guided segmentation models and outperforms BUCTD and BMPv1 by significant margin.

3D Human Pose and Shape Estimation has gained significant attention in recent years [57]. Most methods rely on SMPL-based body models [58, 59], though several alternatives exist. SMIL [60] extends SMPL to infants. ANNY [61] models population-level variability across race, age, and body type. SKEL [62] augments SMPL with a realistic skeleton, while MHR [63] and ATLAS [64] model body shape directly around the physical skeleton. While some models (eg. [65]) estimate 3D bodies directly from images, most 3D pose estimation methods require accurate 2D inputs. Earlier approaches [66–68] assume bounding-box-centered crops, whereas recent methods [1, 2] accept prompts such as text or segmentation masks. BMPv2 provides precise and robust 2D predictions, making it well suited for 3D model prompting.

Data: There are various datasets for 2D human pose estimation or instance segmentation. Most notable are COCO [9], MPII [69] or AIC [70]. Datasets such as OCHuman [6] CrowdPose [4] and CIHP [5] focus on multibody problems such as occlusion and self-occlusion. OCHuman is too small for large-scale training and is traditionally used only for evaluation. Furthermore, it contains annotation errors as showed in Sec. 4.1. CrowdPose is big enough for training but is unsuitable for evaluation in multi-dataset setup as it mixes train and test sets of COCO, MPII and AIC. In addition to the pose estimation, other datasets focus on human crowds, e.g. CrowdHuman [3] on detection or CIHP [5] on human parsing. 3D human pose estimation datasets are mostly synthetic [71–73] or lab-captured [74–77] so they do not evaluate performance in-the-wild. Apart from COCO and OCHuman, there is not enough

datasets to evaluate all three tasks (detection, segmentation and pose estimation) on the same dataset. We attempt to improve the situation with OCHuman-Pose in Sec. 4.1. For COCO and related datasets, the evaluation metric is Object Keypoint Similarity (OKS), while Percentage of Correct Keypoints (PCKh) is used for MPII.

3 Method

BMPv1 [7] connects a detector, pose estimator, and segmenter in a self-improving loop. The core idea is mutual consistency between different human-body representations. Each model is conditioned on the others and iteratively refines its predictions.

The detector is conditioned on previously processed instances. After an instance is processed, its mask is blacked out, forcing the detector to ignore it in subsequent iterations. This enables discovery of missed instances, typically in the background, and recovers cases where multiple people collapse into a single detection.

The pose estimator is conditioned on a segmentation mask from the detector or the mask refinement stage. Masks are more precise than bounding boxes and help disentangle individuals under heavy overlap. The pose estimator in BMPv1, MaskPose, is a standard heatmap-based top-down model with mask conditioning.

The final component of BMPv1 is SAM, which refines segmentation masks using previous estimates and predicted poses. BMPv1 proposes a complex strategy for selecting pose-based point prompts. Despite this, mask refinement remains the dominant failure mode.

In this work, we revisit BMP and introduce two improvements. We replace MaskPose with PMPose and SAM2 with SAM-pose2seg. Both are introduced in the following sections. We further introduce a more expensive but more accurate variant, BMP+, and show how BMP integrates with 3D pose estimation.

3.1 PMPose

Human pose estimation is a central element of the BMP loop. It resolves detection ambiguity in crowds by enforcing anatomical constraints (e.g., each person has two arms) and validates detections before mask refinement. Accurate poses

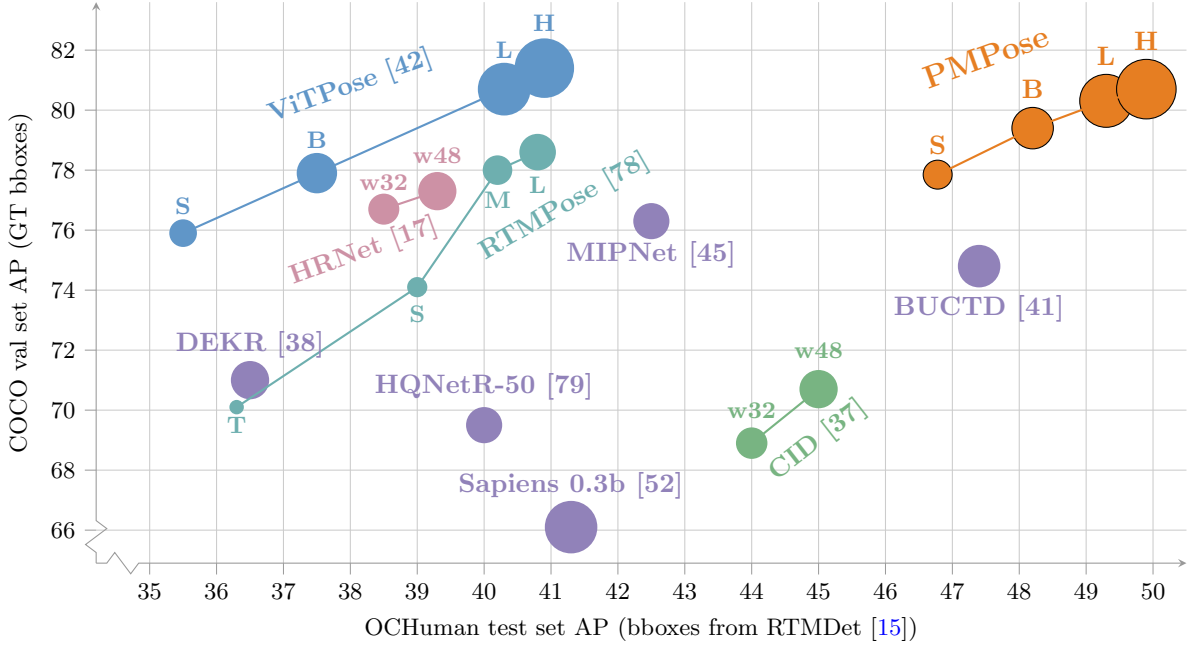


Fig. 2: Comparison of PMPose with state-of-the-art models on the COCO and the OCHuman datasets. The bubble diameter is proportional to a logarithm of number of model parameters. PMPose generalizes the best to unseen OCHuman dataset while keeping SOTA level on COCO.

are critical for the final refinement stage; incorrect joints prevent the separation of overlapping individuals.

The dominant failure modes are (1) merging people when predicted joints belong to multiple individuals and (2) missing disconnected parts, such as the wrists or ankles that are visually detached due to occlusion. BMPv1 uses MaskPose [7], which benefits from mask conditioning and reduces individuals merging. However, MaskPose inherits limitations common in top-down pose estimators. First, because it is trained only on in-image keypoints, it tends to place joints inside the image even when they lie outside, causing instabilities along the bounding box border. Second, its confidence estimates are poorly calibrated. Confidence is crucial for selecting prompts in the mask refinement stage, and overconfident errors lead to incorrect prompt selection that propagates through the pipeline. We address these issues with PMPose (ProbMaskPose), a unified model for pose estimation in BMPv2.

PMPose combines the strengths of MaskPose and ProbPose [10]. It keeps mask conditioning

from MaskPose and adopts the presence probability, visibility estimation, expected OKS prediction, and the resulting border stability from ProbPose. The ViT backbone remains unchanged; only the prediction head and the loss differ.

PMPose follows the same COCO+AIC+MPII training setup as MaskPose and is further finetuned with CropAugmentation on the same datasets. CropAugmentation enables the localization of key points outside the visible region and improves the presence and visibility predictions. For the semi-transparent visibility masking introduced by MaskPose, we use $\alpha = 0.25$ (compared to 0.2 in MaskPose), which is bit-shift friendly and speeds up augmentation.

PMPose has the same outputs as ProbPose [10]: keypoints with calibrated probability maps (\mathcal{K}), presence probability (p_p) indicating whether each joint is present, visibility estimates (v), and expected OKS (\mathbb{E}_{OKS}) as a self-quality measure. All of them are conditioned instance segmentation mask and bounding box as in MaskPose [7]. In the BMP loop, visibility is used to select prompts in pose refinement stage (see

Tab. 6) and \mathbb{E}_{OKS} is used as confidence measure for COCO-style AP evaluation.

We introduce a whole family of models: PMPose-S/B/L/H, paired with ViT-S/B/L/H backbones [80]. The design is consistent across scales; capacity is the only difference. PMPose outperforms ViTPose [42] and improves over MaskPose, especially in crowded scenes (Fig. 2). On COCO, performance matches state-of-the-art levels. PMPose-S provides practical speed for real-time or near-real-time usage, while PMPose-H targets the highest accuracy.

3.2 SAM-`pose2seg`

SAM-`pose2seg` builds on SAM 2.1 [8] and first review the baseline to clarify our modifications.

SAM is trained on a large and diverse dataset, which gives it strong generalization to unseen data. However, SAM lacks explicit semantic understanding. Objects are loosely defined and may correspond to almost arbitrary regions.

Our goal is to preserve SAM’s generalization while specializing it for pose-guided human instance segmentation. We therefore introduce minimal changes and keep most of the original architecture unchanged.

During training, SAM uses point prompts dynamically sampled from the ground-truth mask. For each mask, a single point is uniformly sampled and used to predict a mask. To simulate refinement, an additional points are sampled from the error region, defined as the area where the prediction disagrees with the ground truth. This process is repeated for eight iterations, which results in the behavior observed in BMPv1 [7]: increasing the number of prompt points can degrade performance rather than improve it.

During both training and inference, SAM predicts three candidate masks per prompt. A mask is selected based on the predicted confidence score. This design partially addresses object ambiguity that is not explicitly resolved during the original training procedure.

3.2.1 Adapting SAM for `pose2seg` task

We fine-tune from the original SAM 2.1. The backbone is frozen to preserve generalization. The architecture remains unchanged; only the training procedure is modified.

We adapt the model in two ways.

Human-focused decoder fine-tuning. We fine-tune the decoder to predict only human instances, including clothing as defined by the training annotations. This removes task ambiguity and directly addresses the main failure mode of BMPv1: over-segmentation of skin regions.

Pose-guided prompting during training. We replace random point prompting with pose-aware prompting to inject human keypoint information into the model. The first prompt is the most visible keypoint. In subsequent iterations, we select a keypoint located in the current error region. If no keypoint lies in the error region, we fall back to sampling a random point from that region. As a result, the model learns to operate on pose-driven prompts, which have a different spatial distribution than the random points used in the original SAM training.

This sampling strategy incorporates pose cues directly into training and better aligns the model with pose-guided human segmentation. Training uses human keypoints predicted with ProbPose [10], allowing the use of datasets without keypoint ground truth (CIHP [5]).

Fine-tuning also enables rapid specialization to the human class. Consequently, the complex prompting strategy identified as optimal in BMPv1 is no longer necessary. Selecting a small number of high-visibility keypoints yields comparable or better performance while being significantly simpler. Experiments show that two keypoints are sufficient to characterize an instance; we use three keypoints in the final model for slightly improved performance.

Sec. 5 analyzes how SAM-`pose2seg` improves the BMP loop and its connection to PMPose through visibility and presence probability prediction. Additional ablations are provided in the technical report [11].

3.3 BMP $+$

BMPv1 [7] ablations showed that re-running the pose estimator after mask refinement brought only marginal gains, not justifying the extra computation. This no longer holds for BMPv2. With stronger components—SAM-`pose2seg` for masks and PMPose for pose—looping them yields significant gains. We therefore propose BMPv2+, a higher-performance, higher-cost variant of BMPv2.

Like BMPv2, BMPv2+ starts with instance detection, followed by pose estimation and mask refinement. The key difference is that pose estimation and mask refinement are looped until convergence. In practice, one additional PMPose pass is sufficient, as the second SAM-pose2seg step brings no further gains.

This loop increases computational cost but improves accuracy, particularly for human pose estimation. BMPv2+ is suited for use cases where performance outweighs runtime and resource constraints.

3.4 From 2D to 3D

BMPv1 [7] demonstrated strong robustness in crowded scenes. In BMPv2, we extend this capability to 3D by leveraging reliable 2D masks, boxes, and poses to reason about human bodies under dense interactions. Our goal is to recover accurate 3D poses and shapes despite extreme overlap and occlusion.

BMPv2 uses masks, bboxes, and 2D poses as prompts for a 3D human pose estimator. The 3D step is executed only after the BMP loop converges, as 3D models are computationally heavy. Although 3D estimation could be integrated into the loop similarly to the 2D pose, its cost would make iterative refinement impractical.

The 3D pose predictor encodes the full image once to obtain the image features. For each detected individual, it predicts 3D pose and shape by prompting with the estimated instance’s bbox and mask. This avoids repeated feature extraction and keeps the per-person overhead manageable.

Predicted 3D bodies are filtered using 3D non-maximum suppression. Instance confidence for NMS is inherited from the 2D predictions produced by the BMP loop.

Quantitative results are in Sec. 5.4, with qualitative examples in Fig. 1.

4 Data

BMP targets scenes with very close human interactions where bounding boxes alone cannot separate individuals. Evaluating such models is difficult due to the lack of suitable data. To our knowledge, only CrowdPose [4] and OCHuman [6] focus on human pose estimation in such scenes.

CrowdPose, however, is problematic in multi-dataset training due to data leakage, while Fig. 2 shows that multi-dataset training is essential for strong generalization. This leaves OCHuman as the only viable option, yet we show below that it is insufficient for in-the-wild detection and pose estimation.

The following two sections analyze OCHuman and CIHP datasets, their statistics, how they differ, and what are their weaknesses. We show that annotations in OCHuman are incomplete and, therefore, detection results on the dataset are misleading. To address this gap, we introduce an improved variant of OCHuman, OCHuman-Pose. The dataset will be available on [project website](#).

4.1 OCHuman 2.0

OCHuman was originally created for the pose-to-segmentation task, where the goal is to estimate an instance mask given a human pose. Although

Table 1: The “crowded” datasets: OCHuman, CIHP and the new OCHuman-Pose. $\overline{IoU_{max}}$ is the mean of IoU_{max} over all instances. In OCHuman-Pose, more than 50% of previously un-annotated instances are added to OCHuman images. CIHP is less crowded (see Fig. 3) but larger and its masks are more precise.

	OCH		OCH-Pose		CIHP val
	val	test	val	test	
# imgs	2 500	2 231	2 500	2 231	5 000
# kpts	4 291	3 819	6 546	5 863	0
# masks	4 291	3 819	4 291	3 819	17 520
$\overline{IoU_{max}}$	0.545	0.546	0.527	0.527	0.209

Table 2: ViTPose*-b [42] performance on OCHuman and new OCHuman-Pose using GT bounding boxes (top) and RTMDet [15] (bottom) bounding boxes as input. Missing annotations in OCHuman are evaluated as detection errors (false positives), masking pose estimation errors. On OCHuman-Pose, performance for GT and detected bboxes are much closer, which aligns with qualitative analysis.

GT bboxes	OCHuman		OCHuman-Pose	
	val AP	test AP	val AP	test AP
✓	90.9	91.0	86.4	86.2
✗	44.5	44.1	75.3	76.1

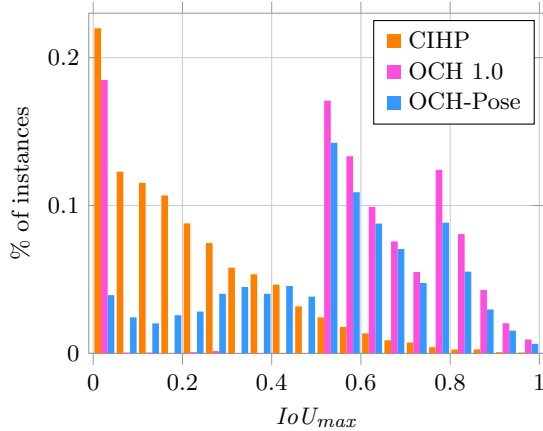


Fig. 3: Instance density measured by IoU_{max} in OCHuman, OCHuman-Pose and CIHP datasets. Despite having almost the same mean of IoU_{max} as OCHuman (Tab. 1), OCHuman-Pose has a more realistic distribution of in-the-wild images, free from artificial instance selections. CIHP has different distribution due to focusing on crowds instead of human interactions.



Fig. 4: Missing annotations in OCHuman. The originally annotated instances are often in the background, which causes problems in COCO-style AP evaluation. OCHuman-Pose expands the original dataset with new instances and previously ignored annotations.

not designed for general-purpose pose estimation, it became the de-facto benchmark for in-the-wild crowded human pose estimation due to the absence of better alternatives.

The main issue with OCHuman is that many individuals are not annotated. For each person, the dataset defines IoU_{max} as the maximum IoU with any other instance in the image. The authors kept only cases with $IoU_{max} = 0$ or $IoU_{max} > 0.5$, excluding all instances with intermediate overlap ($0 < IoU_{max} \leq 0.5$), as shown in Fig. 3. This filtering leaves numerous unannotated people, often

placing the annotated subjects in the background, as shown in Fig. 4.

The COCO-style mAP evaluation [9] sorts the predictions by confidence and assigns the ground truth greedily. Any prediction that ranks first without a matching annotation becomes a false positive. On OCHuman, this forces models to assign the highest confidence to the annotated instance, even when it is not the most prominent person in the image. As illustrated in Fig. 4, there is no reason for these annotated individuals – often in the background – to receive the highest confidence, yet the evaluation protocol penalizes any alternative.

We address this issue by annotating all missing instances with keypoints. As shown in Fig. 4, some individuals had keypoints in the original OCHuman annotations but were excluded due to the dataset’s filtering scheme. We reinstate these annotations and add manual annotations for all instances that lacked them.

Tab. 1 summarizes the statistics of the revised dataset. OCHuman-Pose adds over 50% new instances to the original images. Although the average IoU_{max} remains similar, the distribution now better reflects in-the-wild conditions (Fig. 3): the number of isolated cases with $IoU_{max} = 0$ is reduced and the previously missing range $0 < IoU_{max} \leq 0.5$ is now represented. Measuring pose estimation performance on OCHuman-Pose reflects reality more accurately than the original OCHuman as shown in Tab. 2.

Note that OCHuman-Pose does not include masks for the newly added persons, and thus cannot be used to evaluate segmentation mAP.

4.2 CIHP

Because OCHuman-Pose lacks masks and the original OCHuman annotates only a subset of instances, we require an additional dataset for evaluating instance segmentation in crowded scenes. CIHP contains dense crowds rather than close-contact interactions, leading to different bounding-box overlap patterns (see IoU_{max} distribution in Fig. 3). It is substantially larger than OCHuman and provides more precise masks, but it has no pose annotations and includes some borderline cases (e.g., tiny head fragments).

Since CIHP is a different domain than OCHuman, we report segmentation results on both.

Table 3: Pose estimation – comparison with state-of-the-art. Best results in bold; second best underlined. \ddagger results not reported. \dagger uses a different detector. \P ignores *small* instances in COCO. Summary: PMPose improves MaskPose and sets the new SOTA for top-down approaches. BMPv2 improves BMPv1 [7] and BMPv2+ significantly outperforms the previous SOTA.

Model	OCHuman		OCHuman-Pose		COCO val AP
	val AP	test AP	val AP	test AP	
Methods without explicit detector (single stage + bottom-up)					
DEKR [38]	37.9	36.5	— \ddagger	— \ddagger	71.0
HQNet R-50 \P [79]	— \ddagger	40.0	— \ddagger	— \ddagger	69.5
CID-w48 [37]	46.1	45.0	— \ddagger	— \ddagger	68.9
BUCTD [41]	48.3	47.4	— \ddagger	— \ddagger	74.8
Top-down methods; bounding boxes from RTMDet-l [15]					
Sapiens 0.3b [52]	42.0	41.3	69.8	70.5	66.1
MIPNet \dagger [45]	42.0	42.5	— \ddagger	— \ddagger	76.3
ViTPose-B [42]	37.6	37.5	66.9	67.8	76.4
ViTPose*-B [42]	44.5	44.1	75.3	76.1	77.3
MaskPose-B [7]	46.6	46.6	77.1	78.0	76.8
PMPose-B	47.9	48.2	78.9	80.0	76.9
Iterative methods					
BUCTD 2 \times [41]	48.8	48.3	— \ddagger	— \ddagger	— \ddagger
BMPv1 2 \times [7]	48.7	49.2	79.0	79.9	76.5
BMPv2 2 \times	51.3	51.5	82.4	83.4	78.8
BMPv2+ 2 \times	55.8	55.8	85.8	86.8	78.1

5 Experiments

Unless stated otherwise, we use the following models. RTMDet-L from [7] is used for detection.

PMPose-B is used for human pose estimation. It is trained on a mixture of COCO [9], MPII [69], and AIC [70]. For MPII and AIC, segmentation masks are generated using SAM2.1 [8] with ground-truth bounding boxes and poses as prompts. Mask augmentation is critical for generalization and robustness to detected masks.

SAM-*pose2seg* is built on a SAM-hiera-B+ backbone with our adaptation (see Sec. 3.2). It is fine-tuned on COCO and CIHP [5]. Since CIHP training data lacks pose annotations, pseudo ground-truth poses are generated using an earlier PMPose-B variant together with ground-truth segmentation masks.

Training details (e.g., schedules and learning rates) along with training scripts for reproducibility will be provided on the [project website](#).

5.1 2D Pose Estimation

Tab. 3 compares BMPv2 with the state-of-the-art in crowded human pose estimation. We show a comparison on the OCHuman dataset for comparison with previous approaches. More reliable comparison is on OCHuman-Pose with fixed annotations as explained in Sec. 4.1. Lastly, COCO dataset performance is shown to compare in non-crowded scenarios.

Our new top-down method, PMPose-B, significantly outperforms the state-of-the-art among top-down methods in crowded scenes while keeping performance on COCO. PMPose has performance comparable to BUTCD [41], which is an iterative method. As shown in Fig. 2, PMPose is superior to compared pose models, setting a new state-of-the-art.

BMPv2 outperforms BMPv1 [7] in all measures on all datasets. BMPv2+ is even better and is the first method to exceed 50 AP and 80 AP performance on the OCHuman test and the OCHuman-Pose test, respectively.

Table 4: Detection and segmentation – comparison with state-of-the-art. Best results in bold; second best underlined. \ddagger results not reported. BMPv2 improves BMPv1 [7] especially in instance segmentation thanks to SAM-pose2seg. BMPv2+ results are the same as BMPv2 as the ‘plus’ version is different only by additional PMPose iteration.

Model	OCHuman				OCHuman-Pose		CIHP	
	val AP		test AP		val AP	test AP	val AP	mask
bbox	mask	bbox	mask	bbox	bbox	bbox	mask	
Detectors								
HRNet [17]	27.4	19.9	27.1	19.4	39.1	39.8	65.2	58.7
ConvNeXt [18]	29.2	19.8	29.4	20.4	41.4	42.2	69.1	60.5
HQNet R-50 [79]	30.6	31.5	29.5	31.1	— \ddagger	— \ddagger	— \ddagger	— \ddagger
CoDETR SWIN-L [12]	29.0	— \ddagger	29.6	— \ddagger	41.6	42.5	73.5	— \ddagger
RTMDet-1 [15]	31.1	27.1	30.0	26.2	45.7	45.7	69.5	63.9
Pose-guided segmentation methods								
Occlusion C&P [81]	— \ddagger	28.9	— \ddagger	28.3	— \ddagger	— \ddagger	— \ddagger	— \ddagger
ExPoSeg [29]	— \ddagger	26.4	— \ddagger	26.8	— \ddagger	— \ddagger	— \ddagger	— \ddagger
Crowd-SAM [32]	— \ddagger	31.4	— \ddagger					
Iterative methods								
BMPv1 2x [7]	<u>36.3</u>	<u>33.7</u>	<u>35.9</u>	<u>34.0</u>	49.0	48.8	69.7	65.9
BMPv2 2x	37.6	40.9	37.5	41.1	50.4	51.3	68.8	69.5

BMPv2+ has slightly worse results on COCO compared to BMPv2 for two reasons. One, COCO contains many small instances (more than 30% of instances have a bbox size smaller than 100px). Mask refinement is not suitable for such small instances (most pose-guided segmentation methods such as [6, 29] ignore small instances in evaluation) and looping SAM-pose2seg with PMPose pronounces the error. Second, COCO contains annotation errors along the bounding box edges as shown in [10]. Therefore, ProbPose-like trained PMPose performs poorly on such keypoints.

The last trend worth mentioning is the performance difference between OCHuman and OCHuman-Pose. By annotating missing instances, the performance measure better corresponds to reality and shows gap between detection error and pose estimation error. BMPv2+ has almost the same performance as ViTPose with GT bboxes (85.8 vs. 86.4) on val set and even outperforms ViTPose with GT bboxes on the test set (86.8 vs. 86.2). The results of ViTPose with GT bboxes is in Tab. 2. These results suggest that with BMP loop, the problem of detection in crowded scenarios is largely solved and most of the errors in OCHuman-Pose are from wrong pose estimation, no detection.

5.2 Detection and Segmentation

Comparison with SOTA on detection and instance segmentation is in Tab. 4. The first part of the table shows standard detectors, middle part are pose-guided instance segmentation models and bottom part is comparison with BMPv1.

BMPv2 again outperforms BMPv1 in all measures. The most dramatic increase in instance segmentation thanks to improved SAM-pose2seg.

The only measure where BMP is not SOTA are CIHP bounding boxes. Here BMPv2 even underperforms BMPv1. The improved SAM-pose2seg is built for images with higher resolution and instances of people. CIHP contains small instances similarly to COCO. Further, CIHP contains a lot of instances where only very small part of the person is visible (eg. top of the head and no keypoints). For masks on CIHP, BMPv2 is the best because the mask improvement for bigger instances outweighs wrongly detected small bounding boxes.

Since BMPv2+ converges after second run on PMPose (as explained in Sec. 3.3), its results for detection and instance segmentation are the same as BMPv2.

Table 5: Ablation of BMP components. SAM-pose2seg improves mask AP, PMPose helps pose AP. SAM-pose2seg and PMPose in BMPv2+ brings dramatic pose improvements. BMPv1 with PMPose gives worse segmentation than standalone BMPv1, as the original prompting is optimized for MaskPose’s confidence.

BMP version	OCHuman	
	pose AP	mask AP
BMPv1	49.2	34.0
BMPv1 + SAM-pose2seg	49.5	40.0
BMPv1 + PMPose	50.2	30.8
BMPv2	51.5	41.1
BMPv2+	55.8	41.1

5.3 Ablation Study

Tab. 5 shows contribution of SAM-pose2seg, PMPose and the ‘plus’ version. As expected, SAM-pose2seg improves instance segmentation even for BMPv1 due to its human-focused finetuning. Similarly, PMPose improves pose estimation even in BMPv1.

The most dramatic improvement is BMPv2+ which loops SAM-pose2seg and PMPose. Improvements in both models add more than 4 AP points on pose estimation.

Note that when SAM-pose2seg is used in BMPv1, it is prompted with BMPv1’s complex prompt selection method for fair comparison. Since MaskPose [7] does not predict visibility, using BMPv2 prompting method would bring unfairly bad results.

5.3.1 Visibility Estimation for SAM-pose2seg

Tab. 6 shows how SAM 2.1 [8] and SAM-pose2seg behave when prompted with different keypoints. PMPose predicts (1) presence probability, (2) expected OKS and (3) visibility for each keypoint. All three variables, along with MaskPose’s confidence [7] can be used to select keypoints for prompting. In the experiment, SAM-pose2seg was fine-tuned for each variable for fair comparison. As shown in Tab. 6, PMPose’s visibility is the best predictor of keypoints usefulness. PMPose is useful not only for improved localization but also because the info it provides about each keypoint could be used to better select prompts.

Table 6: SAM prompting with keypoints selected by different metrics. For SAM [8], prompts are chosen using the prompting strategy from [7], whereas SAM-pose2seg uses the top-3 points per metric. These configurations correspond to the optimal settings for each model. For confidence[†], MaskPose [7] was used as PMPose does not return confidence. Visibility is the best predictor of keypoints prompting usefulness.

Metric	COCO	OCH	CIHP
	val AP	test AP	val AP
SAM 2.1			
conf. [†]	32.7	24.6	58.6
pres. prob.	<u>38.2</u>	23.0	61.8
exp. OKS	35.4	<u>25.3</u>	<u>64.5</u>
vis.	41.2	29.5	71.6
SAM-pose2seg			
conf. [†]	38.3	<u>33.6</u>	66.6
pres. prob.	43.8	31.0	69.3
exp. OKS	<u>43.9</u>	34.7	<u>72.0</u>
vis.	44.6	34.7	72.7

5.4 3D Pose Estimation

Tab. 7 proves that BMP is suitable for SAM-3D-Body [1] prompting. SAM-3D-Body needs prompt for mesh reconstruction. The prompt could be bounding box, mask or 2D pose. Our experiments showed that pose does not help nearly as much as segmentation masks. When SAM-3D-Body is prompted with BMPv2 masks, predicted 3D meshes are of comparable quality to 2D poses. This suggests that precise masks simplify both 2D and 3D pose estimation in crowds.

Note that Tab. 7 measures the reprojection of 3D keypoints back to the 2D image, as there is no 3D ground truth for extremely crowded scenarios such as OCHuman. The reprojection measure is good enough to measure the crude correctness of the pose but cannot measure the depth ambiguity. But depth ambiguity is usually not that big problem in multi-body interactions as much as correct assignment of limbs to individuals. Qualitative examples are in Figs. 1 and 6.

5.5 Robustness to Domain Shift

We evaluate BMP generalization on an unseen private dataset from [82]. The most challenging subset involve close adult–infant interactions, where standard pose estimators struggle to separate individuals. The dataset is further challenging

Table 7: Comparison of prompting methods for SAM-3D-body [1] on OCHuman test. Pose AP is reprojection error of the 3D pose. Prompting with BMPv2 gives significantly better 3D poses thanks to much better instance masks.

Detector	masks	OCHuman 3D pose AP	OCH-Pose 3D pose AP
ViTDet-H [16]	✗	36.8	59.6
RTMDet-L [15]	✗	38.5	68.0
BMP [7]	✗	<u>39.9</u>	<u>68.3</u>
BMPv2	✗	46.4	75.8
RTMDet-L [15]	✓	40.0	69.5
BMP [7]	✓	<u>45.6</u>	<u>74.9</u>
BMPv2	✓	54.8	85.2

because (1) adults are often only partially visible, which degrades performance of top-down methods, and (2) infants are absent from standard training sets, causing a strong domain shift. Due to privacy constraints, infant datasets are rarely shared, and models are typically not trained on infants. As the dataset is private, none of the evaluated models – including SAM – were trained on its images, resulting in substantial domain shift.

Tab. 8 and Fig. 5 report quantitative and qualitative results on the challenging lap subset. Both BMPv1 and BMPv2 significantly outperform off-the-shelf SOTA (RTMDet [15] + ViTPose [42]). PMPose, through probabilistic modeling, correctly predicts keypoints outside the image and avoids mixing individuals. The dominant failure mode is missed detections in some frames rather than incorrect association. Since evaluation is frame-based, such failures could be mitigated with temporal consistency in video.

BMPv2 achieves strong performance in complex multi-body scenes and is suitable when accuracy is the primary goal. For time-constrained applications, PMPose, especially PMPose-s, offers a favorable trade-off between accuracy and speed.

6 Conclusions

We present BBoxMaskPose v2 (BMPv2), an improved version of the BBoxMaskPose loop [7]. Performance gains come from a stronger 2D pose estimator, PMPose, and a pose-guided adaptation of SAM for human instance segmentation, SAM-
pose2seg. BMPv2 outperforms BMPv1 across all metrics. It is the first method to exceed 50 AP

Table 8: Robustness to domain shift on a non-public application dataset from [82]. PMPose performs similarly to ViTPose* [42] while providing more information about each keypoint. Both BMPv1 [7] and BMPv2 significantly improve over top-down methods. The private dataset guarantees that the data are from an unseen domain.

Method	pose AP
RTMDet-l [15] + ViTPose-B [42]	73.3
RTMDet-l [15] + ViTPose*-B [42]	76.9
RTMDet-l [15] + PMPose-B	76.4
BMPv1 2× [7]	<u>83.2</u>
BMPv2 2×	83.3

on OCHuman and also maintains state-of-the-art performance on COCO.

Key findings are:

1. Unifying MaskPose [7] and ProbPose [10] yields PMPose, a more accurate and expressive model. PMPose improves state-of-the-art performance in both standard and crowded settings.
2. Adapting SAM [8] for pose-guided human instance segmentation (SAM-
pose2seg) significantly improves the BMP loop, beyond mask precision alone.
3. Improvements from PMPose and SAM-
pose2seg enable an additional pose–mask refinement loop, forming BMPv2+. Pose estimation improves substantially, as the second PMPose iteration operates on masks refined by SAM-
pose2seg.
4. Poor performance on OCHuman [6] is caused by missing annotations. The proposed OCHuman-Pose dataset adds previously ignored instances to better reflect real crowded scenes. On OCHuman-Pose, models using ground-truth and detected boxes show similar performance, unlike the original benchmark, indicating that pose estimation, not detection, is the main bottleneck.
5. Robust 2D prompts are key for accurate 3D human pose estimation in crowded scenes. With BMPv2, state-of-the-art prompted 3D models remain effective on OCHuman even under severe instance overlap.

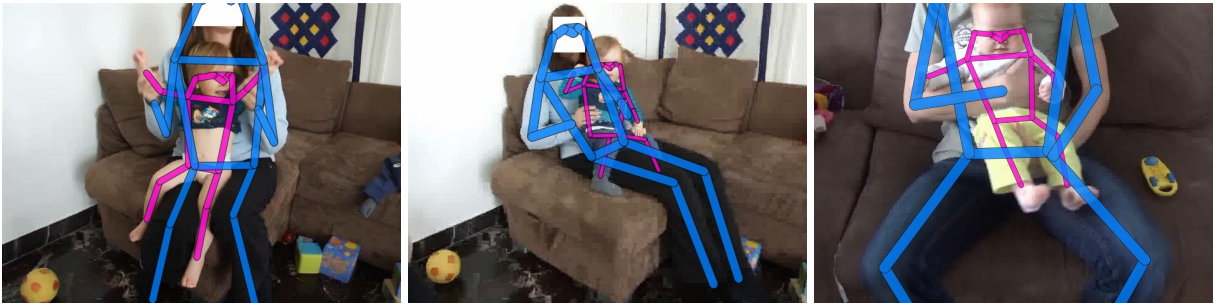


Fig. 5: BMPv2 results on a non-public dataset from [82]. It is able to correctly disentangle individuals even in an unseen domain. Thanks to PMPose, keypoints outside of the image are not predicted inside. Results are shown only for authorized scenes; the dataset itself is more diverse than these examples. Infants anonymized with BLANKET [83].



Fig. 6: Additional qualitative results from OCHuman.

Acknowledgements. This work was supported by the Ministry of the Interior of the Czech Republic project No. VJ02010041, the Technology Agency of the Czech Republic project CEDMO 2.0 No. FW10010387, the European Union’s Digital Europe Programme under Contract No. 101158609, and the Czech Technical University student grant SGS23/173/OHK3/3T/13.

References

- [1] Yang, X., Kukreja, D., Pinkus, D., Sagar, A., Fan, T., Park, J., Shin, S., Cao, J., Liu, J., Ugrinovic, N., Feiszli, M., Malik, J., Dollar, P., Kitani, K.: Sam 3d body: Robust full-body human mesh recovery. Technical report, Meta Superintelligence Labs (2025)
- [2] Wang, Y., Sun, Y., Patel, P., Daniilidis, K., Black, M.J., Kocabas, M.: Prompthmr: Promptable human mesh recovery. In: Proceedings of the Computer Vision and Pattern Recognition Conference, pp. 1148–1159 (2025)
- [3] Shao, S., Zhao, Z., Li, B., Xiao, T., Yu, G., Zhang, X., Sun, J.: Crowdhuman: A benchmark for detecting human in a crowd. ArXiv **abs/1805.00123** (2018)
- [4] Li, J., Wang, C., Zhu, H., Mao, Y., Fang, H.-S., Lu, C.: Crowdpose: Efficient crowded scenes pose estimation and a new benchmark. In: Proceedings of the IEEE/CVF Conference on Computer Vision and Pattern Recognition (CVPR) (2019)
- [5] Gong, K., Liang, X., Li, Y., Chen, Y., Yang, M., Lin, L.: Instance-level human parsing via part grouping network. In: Proceedings of the European Conference on Computer Vision (ECCV), pp. 770–785 (2018)
- [6] Zhang, S.-H., Li, R., Dong, X., Rosin, P., Cai, Z., Han, X., Yang, D., Huang, H., Hu, S.-M.: Pose2seg: Detection free human instance segmentation. In: Proceedings of the IEEE/CVF Conference on Computer Vision and Pattern Recognition, pp. 889–898 (2019)
- [7] Purkrabek, M., Matas, J.: Detection, pose estimation and segmentation for multiple bodies: Closing the virtuous circle. In: Proceedings of the IEEE/CVF International Conference on Computer Vision (ICCV), pp. 9004–9013 (2025)
- [8] Ravi, N., Gabeur, V., Hu, Y.-T., Hu, R., Ryali, C., Ma, T., Khedr, H., Rädle, R., Rolland, C., Gustafson, L., Mintun, E., Pan, J., Alwala, K.V., Carion, N., Wu, C.-Y., Girshick, R., Dollar, P., Feichtenhofer, C.: SAM 2: Segment anything in images and videos. In: The Thirteenth International Conference on Learning Representations (2025)
- [9] Lin, T.-Y., Maire, M., Belongie, S.J., Hays, J., Perona, P., Ramanan, D., Dollár, P., Zitnick, C.L.: Microsoft coco: Common objects in context. In: European Conference on Computer Vision (2014)
- [10] Purkrabek, M., Matas, J.: ProbPose: A probabilistic approach to 2d human pose estimation. In: Proceedings of the Computer Vision and Pattern Recognition Conference (CVPR), pp. 27124–27133 (2025)
- [11] Kolomiiets, C., Purkrabek, M., Matas, J.: Sam-pose2seg: Pose-guided human instance segmentation in crowds. arXiv preprint arXiv:2601.08982 (2026)
- [12] Zong, Z., Song, G., Liu, Y.: Detrs with collaborative hybrid assignments training. In: Proceedings of the IEEE/CVF International Conference on Computer Vision, pp. 6748–6758 (2023)
- [13] Ge, Z.: Yolox: Exceeding yolo series in 2021. arXiv preprint arXiv:2107.08430 (2021)
- [14] Redmon, J., Farhadi, A.: Yolov3: An incremental improvement. arXiv preprint arXiv:1804.02767 (2018)
- [15] Lyu, C., Zhang, W., Huang, H., Zhou, Y., Wang, Y., Liu, Y., Zhang, S., Chen, K.: Rtdet: An empirical study of designing real-time object detectors. ArXiv **abs/2212.07784** (2022)

[16] Li, Y., Mao, H., Girshick, R., He, K.: Exploring plain vision transformer backbones for object detection. In: European Conference on Computer Vision, pp. 280–296 (2022). Springer

[17] Sun, K., Xiao, B., Liu, D., Wang, J.: Deep high-resolution representation learning for human pose estimation. In: Proceedings of the IEEE Conference on Computer Vision and Pattern Recognition, pp. 5693–5703 (2019)

[18] Liu, Z., Mao, H., Wu, C.-Y., Feichtenhofer, C., Darrell, T., Xie, S.: A convnet for the 2020s. Proceedings of the IEEE/CVF Conference on Computer Vision and Pattern Recognition (CVPR) (2022)

[19] Papandreou, G., Zhu, T.L., Kanazawa, N., Toshev, A., Tompson, J., Bregler, C., Murphy, K.P.: Towards accurate multi-person pose estimation in the wild. 2017 IEEE Conference on Computer Vision and Pattern Recognition (CVPR), 3711–3719 (2017)

[20] Ren, T., Liu, S., Zeng, A., Lin, J., Li, K., Cao, H., Chen, J., Huang, X., Chen, Y., Yan, F., et al.: Grounded sam: Assembling open-world models for diverse visual tasks. arXiv preprint arXiv:2401.14159 (2024)

[21] Cuttano, C., Trivigno, G., Rosi, G., Masone, C., Averta, G.: Samwise: Infusing wisdom in sam2 for text-driven video segmentation. In: Proceedings of the Computer Vision and Pattern Recognition Conference, pp. 3395–3405 (2025)

[22] Wei, Z., Chen, P., Yu, X., Li, G., Jiao, J., Han, Z.: Semantic-aware sam for point-prompted instance segmentation. In: Proceedings of the IEEE/CVF Conference on Computer Vision and Pattern Recognition (CVPR), pp. 3585–3594 (2024)

[23] Xiao, S., Kabra, R., Li, Y., Lee, D., Carreira, J., Panda, P.: Openworldsam: Extending sam2 for universal image segmentation with language prompts. arXiv preprint arXiv:2507.05427 (2025)

[24] Azarian, K., Das, D., Park, H., Porikli, F.: Test-time adaptation vs. training-time generalization: A case study in human instance segmentation using keypoints estimation. In: Proceedings of the IEEE/CVF Winter Conference on Applications of Computer Vision, pp. 411–420 (2023)

[25] Azarian, K., Das, D., Park, H., Porikli, F.M.: Test-time adaptation vs. training-time generalization: A case study in human instance segmentation using keypoints estimation. 2023 IEEE/CVF Winter Conference on Applications of Computer Vision Workshops (WACVW), 411–420 (2022)

[26] Li, Z., Chen, X., Zhou, W., Zhang, Y., Yu, J.: Pose2body: Pose-guided human parts segmentation. In: 2019 IEEE International Conference on Multimedia and Expo (ICME), pp. 640–645 (2019). <https://doi.org/10.1109/ICME.2019.00116>

[27] Tripathi, S., Collins, M.D., Brown, M.A., Belongie, S.J.: Pose2instance: Harnessing keypoints for person instance segmentation. ArXiv **abs/1704.01152** (2017)

[28] Ahmad, N., Khan, J., Kim, J.Y., Lee, Y.: Joint human pose estimation and instance segmentation with poseplusseg. In: AAAI Conference on Artificial Intelligence (2022)

[29] Zhou, D., He, Q.: Poseg: Pose-aware refinement network for human instance segmentation. IEEE Access **8**, 15007–15016 (2020) <https://doi.org/10.1109/ACCESS.2020.2967147>

[30] Ahmad, N., Khan, J., Kim, J.Y., Lee, Y.: Multiposeseg: Feedback knowledge transfer for multi-person pose estimation and instance segmentation. 2022 26th International Conference on Pattern Recognition (ICPR), 2086–2092 (2022)

[31] Yang, L., Song, Q., Wang, Z., Jiang, M.: Parsing r-cnn for instance-level human analysis. In: Proceedings of the IEEE Conference on Computer Vision and Pattern Recognition (CVPR) (2019)

[32] Cai, Z., Gao, Y., Zheng, Y., Zhou, N., Huang, D.: Crowd-sam: Sam as a smart annotator for object detection in crowded scenes. In: Proceedings of the European Conference on Computer Vision (ECCV) (2024)

[33] Oquab, M., Dariseti, T., Moutakanni, T., Vo, H.V., Szafraniec, M., Khalidov, V., Fernandez, P., HAZIZA, D., Massa, F., El-Nouby, A., Assran, M., Ballas, N., Galuba, W., Howes, R., Huang, P.-Y., Li, S.-W., Misra, I., Rabbat, M., Sharma, V., Symnaeve, G., Xu, H., Jegou, H., Mairal, J., Labatut, P., Joulin, A., Bojanowski, P.: DINOv2: Learning robust visual features without supervision. Transactions on Machine Learning Research (2024). Featured Certification

[34] Stoffl, L., Vidal, M., Mathis, A.: End-to-end trainable multi-instance pose estimation with transformers. arXiv preprint arXiv:2103.12115 (2021)

[35] Shi, D., Wei, X., Li, L., Ren, Y., Tan, W.: End-to-end multi-person pose estimation with transformers. In: Proceedings of the IEEE/CVF Conference on Computer Vision and Pattern Recognition, pp. 11069–11078 (2022)

[36] Xiao, Y., Wang, X., Yu, D., Su, K., Jin, L., Song, M., Yan, S., Zhao, J.: Adaptive-pose++: A powerful single-stage network for multi-person pose regression. arXiv preprint arXiv:2210.04014 (2022)

[37] Wang, D., Zhang, S.: Contextual instance decoupling for robust multi-person pose estimation. 2022 IEEE/CVF Conference on Computer Vision and Pattern Recognition (CVPR), 11050–11058 (2022)

[38] Geng, Z., Sun, K., Xiao, B., Zhang, Z., Wang, J.: Bottom-up human pose estimation via disentangled keypoint regression. In: Proceedings of the IEEE/CVF Conference on Computer Vision and Pattern Recognition (CVPR), pp. 14676–14686 (2021)

[39] Cao, Z., Simon, T., Wei, S.-E., Sheikh, Y.: Realtime multi-person 2d pose estimation using part affinity fields. In: Proceedings of the IEEE Conference on Computer Vision and Pattern Recognition, pp. 7291–7299 (2017)

[40] Papandreou, G., Zhu, T.L., Chen, L.-C., Gidaris, S., Tompson, J., Murphy, K.P.: Personlab: Person pose estimation and instance segmentation with a bottom-up, part-based, geometric embedding model. In: European Conference on Computer Vision (2018)

[41] Zhou, M., Stoffl, L., Mathis, M.W., Mathis, A.: Rethinking pose estimation in crowds: overcoming the detection information bottleneck and ambiguity. 2023 IEEE/CVF International Conference on Computer Vision (ICCV), 14643–14653 (2023)

[42] Xu, Y., Zhang, J., Zhang, Q., Tao, D.: ViTPose: Simple vision transformer baselines for human pose estimation. In: Advances in Neural Information Processing Systems (2022)

[43] Liu, Z., Lin, Y., Cao, Y., Hu, H., Wei, Y., Zhang, Z., Lin, S., Guo, B.: Swin transformer: Hierarchical vision transformer using shifted windows. In: Proceedings of the IEEE/CVF International Conference on Computer Vision, pp. 10012–10022 (2021)

[44] Yuan, Y., Fu, R., Huang, L., Lin, W., Zhang, C., Chen, X., Wang, J.: Hrformer: High-resolution vision transformer for dense predict. Advances in neural information processing systems **34**, 7281–7293 (2021)

[45] Khirodkar, R., Chari, V., Agrawal, A., Tyagi, A.: Multi-instance pose networks: Rethinking top-down pose estimation. 2021 IEEE/CVF International Conference on Computer Vision (ICCV), 3102–3111 (2021)

[46] Wang, W., Xie, E., Li, X., Fan, D.-P., Song, K., Liang, D., Lu, T., Luo, P., Shao, L.: Pvt v2: Improved baselines with pyramid vision transformer. Computational Visual Media **8**(3), 415–424 (2022)

[47] Toshev, A., Szegedy, C.: Deeppose: Human pose estimation via deep neural networks. 2014 IEEE Conference on Computer Vision and Pattern Recognition, 1653–1660 (2013)

[48] Sun, X., Shang, J., Liang, S., Wei, Y.: Compositional human pose regression. In: Proceedings of the IEEE International Conference on Computer Vision, pp. 2602–2611 (2017)

[49] Li, J., Bian, S., Zeng, A., Wang, C., Pang, B., Liu, W., Lu, C.: Human pose regression with residual log-likelihood estimation. In: Proceedings of the IEEE/CVF International Conference on Computer Vision, pp. 11025–11034 (2021)

[50] Sun, X., Xiao, B., Wei, F., Liang, S., Wei, Y.: Integral human pose regression. In: Proceedings of the European Conference on Computer Vision (ECCV), pp. 529–545 (2018)

[51] Luvizon, D.C., Tabia, H., Picard, D.: Human pose regression by combining indirect part detection and contextual information. *Computers & Graphics* **85**, 15–22 (2019)

[52] Khirodkar, R., Bagautdinov, T., Martinez, J., Su, Z., James, A., Selednik, P., Anderson, S., Saito, S.: Sapiens: Foundation for human vision models. In: European Conference on Computer Vision (2024)

[53] Wang, Y., Wu, Y., Tang, S., He, W., Guo, X., Zhu, F., Bai, L., Zhao, R., Wu, J., He, T., Ouyang, W.: Hulk: A universal knowledge translator for human-centric tasks. ArXiv **abs/2312.01697** (2023)

[54] Ci, Y., Wang, Y., Chen, M., Tang, S., Bai, L., Zhu, F., Zhao, R., Yu, F., Qi, D., Ouyang, W.: Unihcp: A unified model for human-centric perceptions. 2023 IEEE/CVF Conference on Computer Vision and Pattern Recognition (CVPR), 17840–17852 (2023)

[55] S.A. Ghasemzadeh, A., Van Zandycke, G., Istasse, M., Sayez, N., Moshtaghpoor, A., De Vleeschouwer, C.: Deepssportlab: a unified framework for ball detection, player instance segmentation and pose estimation in team sports scenes. In: 32nd British Machine Vision Conference 2021 (BMVC 2021) (2021)

[56] Rukhovich, D., Sofiuk, K., Galeev, D., Barianova, O., Konushin, A.: Iterdet: iterative scheme for object detection in crowded environments. In: Structural, Syntactic, and Statistical Pattern Recognition: Joint IAPR International Workshops, S+ SSPR 2020, Padua, Italy, January 21–22, 2021, Proceedings, pp. 344–354 (2021). Springer

[57] Tian, Y., Zhang, H., Liu, Y., Wang, L.: Recovering 3d human mesh from monocular images: A survey. *IEEE transactions on pattern analysis and machine intelligence* **45**(12), 15406–15425 (2023)

[58] Loper, M., Mahmood, N., Romero, J., Pons-Moll, G., Black, M.J.: SMPL: A skinned multi-person linear model. *ACM Trans. Graphics (Proc. SIGGRAPH Asia)* **34**(6), 248–124816 (2015)

[59] Pavlakos, G., Choutas, V., Ghorbani, N., Bolkart, T., Osman, A.A.A., Tzionas, D., Black, M.J.: Expressive body capture: 3d hands, face, and body from a single image. In: Proceedings IEEE Conf. on Computer Vision and Pattern Recognition (CVPR) (2019)

[60] Hesse, N., Pujades, S., Romero, J., Black, M.J., Bodensteiner, C., Arens, M., Hofmann, U.G., Tacke, U., Hadders-Algra, M., Weinberger, R., *et al.*: Learning an infant body model from rgb-d data for accurate full body motion analysis. In: International Conference on Medical Image Computing and Computer-Assisted Intervention, pp. 792–800 (2018). Springer

[61] Brégier, R., Fiche, G., Bravo-Sánchez, L., Lucas, T., Armando, M., Weinzaepfel, P., Rogez, G., Baradel, F.: Human mesh modeling for any body. arXiv preprint arXiv:2511.03589 (2025)

[62] Keller, M., Werling, K., Shin, S., Delp, S., Pujades, S., Liu, C.K., Black, M.J.: From skin to skeleton: Towards biomechanically accurate 3d digital humans. *ACM Transactions on Graphics (TOG)* **42**(6), 1–12 (2023)

[63] Ferguson, A., Osman, A.A., Bescos, B., Stoll, C., Twigg, C., Lassner, C., Otte, D., Vignola, E., Bogo, F., Santesteban, I., et al.: Mhr: Momentum human rig. arXiv preprint arXiv:2511.15586 (2025)

[64] Park, J., Romero, J., Saito, S., Prada, F., Shiratori, T., Xu, Y., Bogo, F., Yu, S.-I., Kitani, K., Khirodkar, R.: Atlas: Decoupling skeletal and shape parameters for expressive parametric human modeling. In: Proceedings of the IEEE/CVF International Conference on Computer Vision, pp. 6508–6518 (2025)

[65] Baradel, F., Armando, M., Galaaoui, S., Brégier, R., Weinzaepfel, P., Rogez, G., Lucas, T.: Multi-hmr: Multi-person whole-body human mesh recovery in a single shot. In: European Conference on Computer Vision, pp. 202–218 (2024). Springer

[66] Sárándi, I., Pons-Moll, G.: Neural localizer fields for continuous 3d human pose and shape estimation. Advances in Neural Information Processing Systems **37**, 140032–140065 (2024)

[67] Lin, K., Wang, L., Liu, Z.: End-to-end human pose and mesh reconstruction with transformers. In: Proceedings of the IEEE/CVF Conference on Computer Vision and Pattern Recognition, pp. 1954–1963 (2021)

[68] Lin, K., Wang, L., Liu, Z.: Mesh graphomer. In: Proceedings of the IEEE/CVF International Conference on Computer Vision, pp. 12939–12948 (2021)

[69] Andriluka, M., Pishchulin, L., Gehler, P., Schiele, B.: 2d human pose estimation: New benchmark and state of the art analysis. In: IEEE Conference on Computer Vision and Pattern Recognition (CVPR) (2014)

[70] Wu, J., Zheng, H., Zhao, B., Li, Y., Yan, B., Liang, R., Wang, W., Zhou, S., Lin, G., Fu, Y., Wang, Y., Wang, Y.: Ai challenger : A large-scale dataset for going deeper in image understanding. ArXiv **abs/1711.06475** (2017)

[71] Black, M.J., Patel, P., Tesch, J., Yang, J.: BEDLAM: A synthetic dataset of bodies exhibiting detailed lifelike animated motion. In: Proceedings IEEE/CVF Conf. on Computer Vision and Pattern Recognition (CVPR), pp. 8726–8737 (2023)

[72] Varol, G., Romero, J., Martin, X., Mahmood, N., Black, M.J., Laptev, I., Schmid, C.: Learning from synthetic humans. In: CVPR (2017)

[73] Patel, P., Huang, C.-H.P., Tesch, J., Hoffmann, D.T., Tripathi, S., Black, M.J.: AGORA: Avatars in geography optimized for regression analysis. In: Proceedings IEEE/CVF Conf. on Computer Vision and Pattern Recognition (CVPR) (2021)

[74] Von Marcard, T., Henschel, R., Black, M.J., Rosenhahn, B., Pons-Moll, G.: Recovering accurate 3d human pose in the wild using imus and a moving camera. In: Proceedings of the European Conference on Computer Vision (ECCV), pp. 601–617 (2018)

[75] Ionescu, C., Papava, D., Olaru, V., Sminchisescu, C.: Human3.6m: Large scale datasets and predictive methods for 3d human sensing in natural environments. IEEE Transactions on Pattern Analysis and Machine Intelligence **36**(7), 1325–1339 (2014)

[76] Zhang, T., Huang, B., Wang, Y.: Object-occluded human shape and pose estimation from a single color image. In: Proceedings of the IEEE/CVF Conference on Computer Vision and Pattern Recognition, pp. 7376–7385 (2020)

[77] Joo, H., Liu, H., Tan, L., Gui, L., Nabbe, B., Matthews, I., Kanade, T., Nobuhara, S., Sheikh, Y.: Panoptic studio: A massively multiview system for social motion capture. In: Proceedings of the IEEE International Conference on Computer Vision, pp. 3334–3342 (2015)

[78] Jiang, T., Lu, P., Zhang, L., Ma, N., Han, R., Lyu, C., Li, Y., Chen, K.: Rtmpose: Real-time multi-person pose estimation based on mmpose. arXiv preprint arXiv:2303.07399 (2023)

- [79] Jin, S., Li, S., Li, T., Liu, W., Qian, C., Luo, P.: You only learn one query: learning unified human query for single-stage multi-person multi-task human-centric perception. In: European Conference on Computer Vision, pp. 126–146 (2024). Springer
- [80] Dosovitskiy, A.: An image is worth 16x16 words: Transformers for image recognition at scale. In: Proceedings of the IEEE/CVF Conference on Computer Vision and Pattern Recognition, pp. 45–67 (2021)
- [81] Ling, E., Huang, D.-K., Hur, M.: Humans need not label more humans: Occlusion copy & paste for occluded human instance segmentation. In: British Machine Vision Conference (2022)
- [82] Gama, F., Mísař, M., Navara, L., T. Popescu, S., Hoffmann, M.: Automatic infant 2d pose estimation from videos: comparing seven deep neural network methods. Behavior Research Methods **57**(10), 280 (2025)
- [83] Hadera, D., Cech, J., Purkrabek, M., Hoffmann, M.: Blanket: Anonymizing faces in infant video recordings. In: 2025 IEEE International Conference on Development and Learning (ICDL), pp. 1–8 (2025). IEEE